The Crystal Structure of r(CCCCGGGG) in Two Distinct Lattices†

Stefan Portmann,‡ Nassim Usman,§ and Martin Egli*,‡

Organic Chemistry Laboratory, ETH Swiss Federal Institute of Technology, CH-8092 Zürich, Switzerland, and Ribozyme Pharmaceuticals Inc., 2950 Wilderness Place, Boulder, Colorado 80301

Received March 13, 1995; Revised Manuscript Received April 17, 1995⊗

ABSTRACT: The structure of the RNA octamer r(C_4G_4) has been determined in two different crystal forms. The conformations of the RNA duplex in the rhombohedral and hexagonal lattices display only minimal deviations, demonstrating that the RNA double helix is considerably less deformable than the DNA double helix. For the first time the crystal structures of an A-RNA and an A-DNA with identical sequence can now be compared. The large number of ordered water molecules observed in the minor groove of the RNA duplex suggests that an important contribution to its higher rigidity derives from the improved hydration due to the presence of the 2′-hydroxyl groups. Our finding that the conformation of the RNA double helix is virtually unaffected by different crystal packing modes provides evidence that proteins may not alter the conformation of RNA stem regions in a significant way.

The crystal structures of over 100 synthetic DNA fragments have led to detailed knowledge of the polymorphic nature of the double helix (Kennard & Hunter, 1991; Dickerson, 1992; Egli, 1994). Such studies indicated considerable plasticity of the DNA duplex and demonstrated the dependence of the DNA structure on its crystallographic environment (Shakked *et al.*, 1989; Jain & Sundaralingam, 1989; Lipanov *et al.*, 1993). However, only very few double-helical RNA fragments have been investigated with crystallographic methods to date (Dock-Bregeon *et al.*, 1988; Holbrook *et al.*, 1991; Cruse *et al.*, 1994; Leonard *et al.*, 1994; Baeyens *et al.*, 1995). Thus, our understanding of the influence on RNA structure of base sequence, hydration, and packing forces, among others, is considerably more limited compared with DNA. We report here the crystal structures of a self-complementary RNA octamer with sequence r(C_4G_4) in a rhombohedral and a hexagonal form at resolutions of 1.8 and 2.9 Å, respectively. The different packing modes for the two crystal forms permit the assessment of the conformational dependence of the RNA double helix on its crystallographic environment and hydration state. Contrary to DNA, the investigated RNA double helix exhibits considerable rigidity, and its conformation is virtually unaffected by the crystal environment and particular base sequence characteristics. Moreover, its geometry and overall shape are notably different from those of the A-DNA double helix with identical sequence. The results of this work further our insight into the conformational features of stem regions in large RNA molecules and the interaction modes underlying RNA−RNA and protein−RNA interactions.

MATERIALS AND METHODS

A preliminary description of the experimental procedures has been given elsewhere (Egli *et al.*, 1995). The octamer was chemically synthesized following standard protocols (Scaringe *et al.*, 1990; Usman *et al.*, 1992) and purified by anion-exchange chromatography and reverse-phase HPLC. Optimal crystallization conditions were established with commercially available screening solutions (Crystal Screen, Hampton Research). Crystals were obtained under a wide range of conditions (Egli *et al.*, 1995). The combination of Ca^{2+} ions with either sodium acetate or sodium cacodylate buffer (pH 4.5) and either 2-methyl-2,4-pentanediol (MPD) or 2-propanol as the precipitant resulted in growth of hexagonal crystals. The combination of Ca^{2+} ions with sodium HEPES buffer (pH 7.5) and ammonium sulfate as the precipitant resulted in growth of rhombohedral crystals. However, it appears that it is not the nature of the bivalent metal cation, but rather high concentrations of ammonium sulfate which are essential for growth of the rhombohedral crystal form. The crystals used for data collection were grown under the following conditions: rhombohedral form, 1 mM RNA, 50 mM sodium acetate (pH 4.6), 1 M ammonium sulfate, equilibrated against 100 mM sodium acetate (pH 4.6), and 2 M ammonium sulfate; hexagonal form, 1 mM RNA, 50 mM sodium cacodylate (pH 4.5), 7.8 mM calcium chloride, and 15% MPD, equilibrated against 30% MPD.

Data were collected on a Maresearch image plate system mounted on an Enraf-Nonius rotating anode generator (Cu Kα radiation). Crystal data for both forms are summarized

Table 1: Crystal Data of r(C_4G_4)

	rhombohedral crystal	hexagonal crystal
temperature	RT[a]	RT
space group	*R*32	$P6_122$
a (Å)	42.40	39.74
b (Å)	42.40	39.74
c (Å)	131.70	58.55
volume/base pair (Å^3)	1424	1668
resolution (Å)	1.8	2.9
no. of reflections at $2\sigma(F)$ level	4382	710
R-factor (%)	20.1	25
no. of waters (first shell)	52 (46)	

[a] RT = room temperature.

† The final coordinates for the hexagonal and the rhombohedral crystal form have been deposited in the Brookhaven Protein Data Bank (entry numbers 1RXA and 1RXB, respectively).

* To whom correspondence should be addressed.
‡ ETH Swiss Federal Institute of Technology.
§ Ribozyme Pharmaceuticals Inc.

⊗ Abstract published in *Advance ACS Abstracts,* May 15, 1995.

0006-2960/95/0434-7569$09.00/0

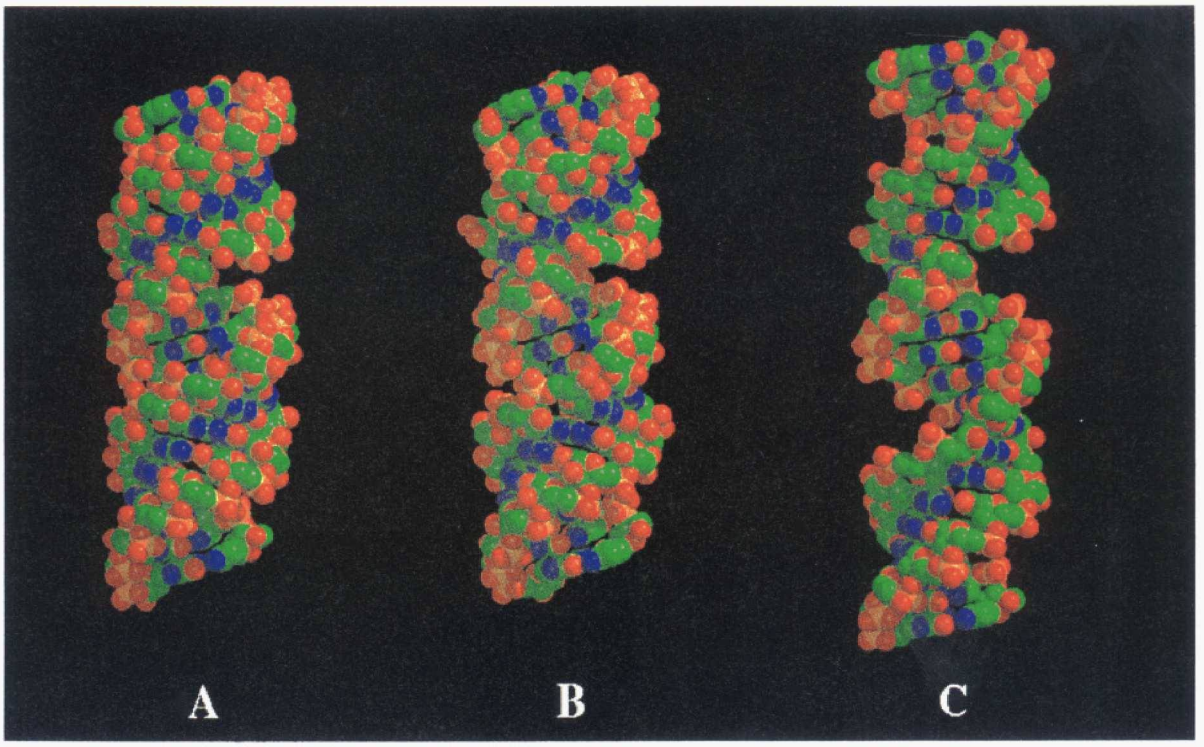

FIGURE 1: Space-filling representations of continuous double helices based on the conformations of the rhombohedral (A) and hexagonal (B) crystal forms of r(C_4G_4), as well as the A-DNA with identical sequence (C). Individual octamers were translated and rotated relative to the corresponding overall helix axis by multiples of the helical parameters presented in Table 2 to generate the 24 base pair long duplexes.

Table 2: Selected Helical Parameters[a] for r(C_4G_4) in Both Lattices and d(C_4G_4)[b]

Overall Parameters (Rise and Widths in Angstroms, Inclination and Twist in Degrees, SD in Parentheses)

structure	inclination	twist	rise	major groove width	minor groove width
r(C_4G_4) rhombohedral	16.6(0.5)	33.0(1.3)	2.5(0.1)	4.2(0.2)	9.8(0.2)
r(C_4G_4) hexagonal	15.5(1.6)	34.0(3.8)	2.5(0.3)	3.3(0.3)	9.7(0.6)
d(C_4G_4)	8.0(0.8)	32.9(3.7)	3.1(0.1)	9.2(0.9)	9.3(0.5)

Selected Local Parameters (Roll and Slide in Angstroms, Twist in Degrees)

	r(C_4G_4) rhombohedral			r(C_4G_4) hexagonal			d(C_4G_4)		
step	roll	slide	twist	roll	slide	twist	roll	slide	twist
C−C	5.6	−1.5	34.1	1.7	−1.8	37.8	6.5	−1.3	35.1
C−C	6.4	−1.7	34.4	2.9	−2.2	34.8	4.4	−2.0	31.7
C−C	7.1	−1.7	32.9	16.3	−2.0	28.7	4.9	−1.5	35.6
C−G	7.9	−2.0	33.3	3.0	−1.5	35.1	−2.0	−2.1	25.4
G−G	11.3	−2.0	30.5	16.3	−2.0	28.7	4.9	−1.5	35.6
G−G	5.4	−1.9	32.9	2.9	−2.2	34.8	4.4	−2.0	31.7
G−G	7.5	−1.8	33.0	1.7	−1.8	37.8	6.5	−1.3	35.1
av	7.3	−1.8	33.0	6.4	−1.9	34.0	4.2	−1.7	32.9
SD	2.0	0.2	1.3	6.8	0.3	3.8	2.9	0.4	3.7

[a] Calculated with the NEWHEL93 program of R. E. Dickerson. [b] Haran *et al.*, 1987; Eisenstein & Shakked, 1995.

in Table 1. Crystal structure determination was first attempted with the hexagonal form, since it was assumed that the duplex would be located on a 2-fold rotation axis, thus facilitating the molecular replacement search. The structure was solved with the program AMoRe (CCP4, 1994; Navaza, 1994), using the A-DNA duplex with identical sequence and added 2′-oxygens as the search model. Refinement was carried out with the programs NUCLSQ (modified for nucleic acids; Quigley *et al.*, 1978) and X-PLOR (Brünger, 1987). The refined structure was then used as the search model for solving the structure of the rhombohedral crystal form. The best solutions proposed by the automatic search routine all showed overlaps between terminal base pairs, and the correct solution yielding optimal stacking interactions between adjacent duplexes was found by manual positioning of the model. The rhombohedral structure was refined with X-PLOR. Positions of water molecules in the rhombohedral crystal form were determined from superimposed sum ($2F_o - F_c$) and difference ($F_o - F_c$) electron density maps, displayed with the program FRODO/TOM on a Silicon Graphics Indigo 2 computer. Temperature factors as well as occupancies of water molecules were refined. In the case of the hexagonal crystal form no water molecules were included in the refinement so far, because of the limited resolution of the data. The final coordinates for the hexagonal and the rhombohedral crystal form have been deposited in the Brookhaven Protein Data Bank.

RESULTS AND DISCUSSION

Overall Conformations. The two conformations of the RNA duplex in the rhombohedral and hexagonal lattices are remarkably similar, with subtle variations only present in the two termini and the central region of the backbones (the RMS deviation between the structures is 0.62 Å). A comparison of the overall shapes of continuous double helices based on the rhombohedral and hexagonal structures is depicted in Figure 1A,B. Selected helical parameters of the three double helices are given in Table 2. As visible, the RNA double helices extrapolated from the rhombohedral and hexagonal structures are practically indistinguishable. Both exhibit the A-form typical inclinations of base pair planes with respect to the helix axis as well as the wide and shallow minor groove paired with a narrow and deep major groove. Consistent with the impression from constructed

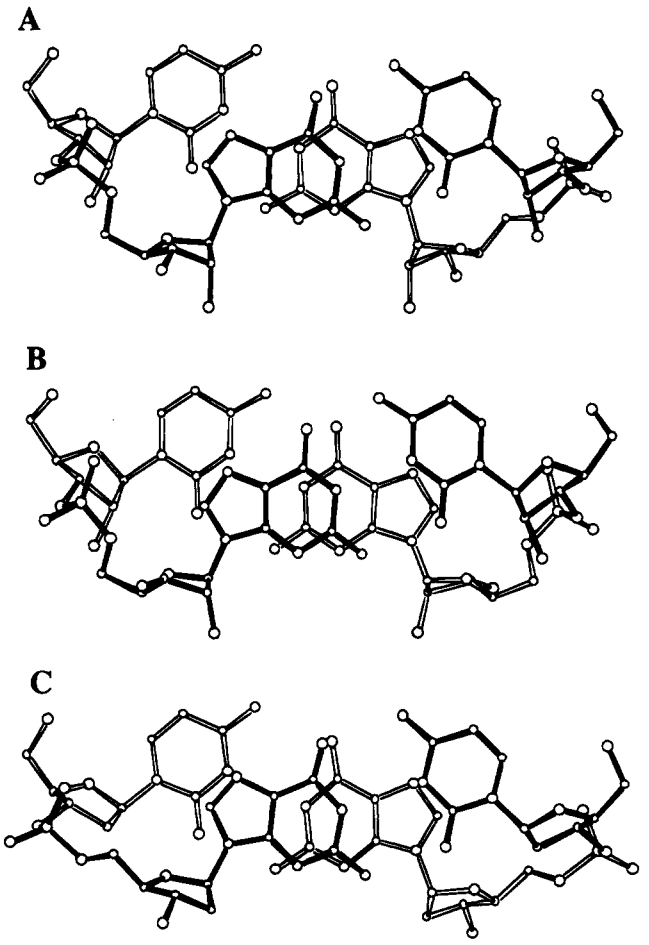

FIGURE 2: Stacking at the central CpG step in the rhombohedral (A) and hexagonal (B) crystal forms of r(C_4G_4), as well as in the A-DNA with identical sequence (C). The projections are along the normal to the best plane through the top base pair (filled bonds).

models are the generally quite similar global helical parameters of the two duplexes. Among the local parameters compared in Table 2, notable deviations between the two duplexes occur mainly with twist angles. The double helix in the hexagonal lattice is constrained by a crystallographic 2-fold rotation axis, whereas it lies in a general position in the rhombohedral lattice. Despite the higher symmetry of the hexagonal duplex, the rhombohedral one appears to be intrinsically more regular. In the latter one, all riboses except for one associated with an extended backbone conformation in the center of the duplex [residue G(13); residues of strand 1 are numbered C(1) to G(8), and residues of strand 2 are numbered C(9) to G(16)] adopt the expected C3′-*endo* pucker. In the hexagonal duplex, certain ribose puckers fall into the two neighboring pseudorotation phase angle ranges C4′-*exo* and C2′-*exo*. However, larger deviations among individual helix parameters for the hexagonal crystal form as indicated by higher standard deviations may be a consequence of the lower resolution of these data to some extent.

Close global resemblance of the RNA duplexes in the two crystal forms does not prevent subtle local conformational differences. This is most evident from a comparison of the backbone conformations in the central CpG steps in the rhombohedral and hexagonal duplexes (Figure 2, Table 3). The backbones in the hexagonal duplex bridging this step have identical geometries due to the crystallographic 2-fold symmetry. All torsion angles fall within the standard A-type

Table 3: Backbone Torsion Angles (Average and Selected Individual Values) and Glycosidic Torsion Angles

torsion angle (deg)	r(C_4G_4) rhombohedral av[a]	SD	central step of strand 2	r(C_4G_4) hexagonal av	SD
α	292.0	4.2	157.5	308.2	55.9
β	172.1	6.2		167.9	13.9
γ	58.4	3.1	177.7	47.6	56.8
δ	76.5	4.1		84.5	15.8
ϵ	208.1	5.2		201.1	24.1
ζ	287.1	5.1		287.4	28.1
χ	197.4	5.9		183.6	9.0

[a] Torsion angles α and γ at the central step of the second strand in the rhombohedral structure were excluded to calculate the average.

duplex ranges, resulting in a compact arrangement of the backbone and an apparently wider turn as visible in the projections of base pairs in Figure 2. In the rhombohedral duplex which is not constrained by crystallographic symmetry, the same central step is bridged by asymmetric backbones. One strand assumes a geometry which is identical to those in the hexagonal duplex (Figure 2A, left). The other adopts an extended conformation with the three torsions to the 5′-side of the phosphate group all lying in the *trans* range and a consequently tighter turn as evident from Figure 2A (right). Such local conformational freedom was first observed in the d(C_4G_4) structure and has been attributed to improved cross-strand stacking (Haran *et al.*, 1987), as well as to packing and hydration effects (Shakked *et al.*, 1989; Jain & Sundaralingam, 1989; Ramakrishnan & Sundaralingam, 1993). For A-DNA octamers considerable untwisting paired with a pronounced slide of base pairs and a central kink was repeatedly observed at central pyrimidine−purine steps. We find that the RNA duplex is much less deformable and that local distortions do not alter the overall structure. The conformational changes in the backbone affect the stacking geometry only minimally. This finding essentially confirms the conclusion that the deformations found for many octameric A-DNA duplexes such as unwinding and kinking at the central base pair step are due to differences in the crystallographic environment. Despite close packing contacts of the rhombohedral RNA duplex, its groove topologies closely resemble those of the hexagonal duplex which enjoys a much less restrictive environment in the crystal (see packing paragraph below). The deformability of the DNA duplex as a result of different packing forces in the crystal is in agreement with the geometrical variations of the DNA duplex in complexes with proteins. Consequently, direct contacts of proteins with RNA may alter the more rigid conformation of stem regions to a lesser extent.

Comparisons with d(C_4G_4). There is a striking difference between the conformations of the rhombohedral and hexagonal RNA double helices on the one hand and the A-DNA duplex with identical sequence on the other (Figure 1). The A-DNA duplex displays a relatively small inclination of base pairs and a wide major groove (Figure 1C, Table 2) and has the appearance of A′-RNA (Saenger, 1984). The DNA duplex is more slim, and its helical rise is extended by 0.6 Å in comparison with the RNA duplexes. DNA duplexes were shown to be quite deformable under the influence of different packing modes, hydration levels, and temperature variations (Wang *et al.*, 1982; Shakked *et al.*, 1989; Jain & Sundaralingam, 1989; Lipanov *et al.*, 1993). The A-

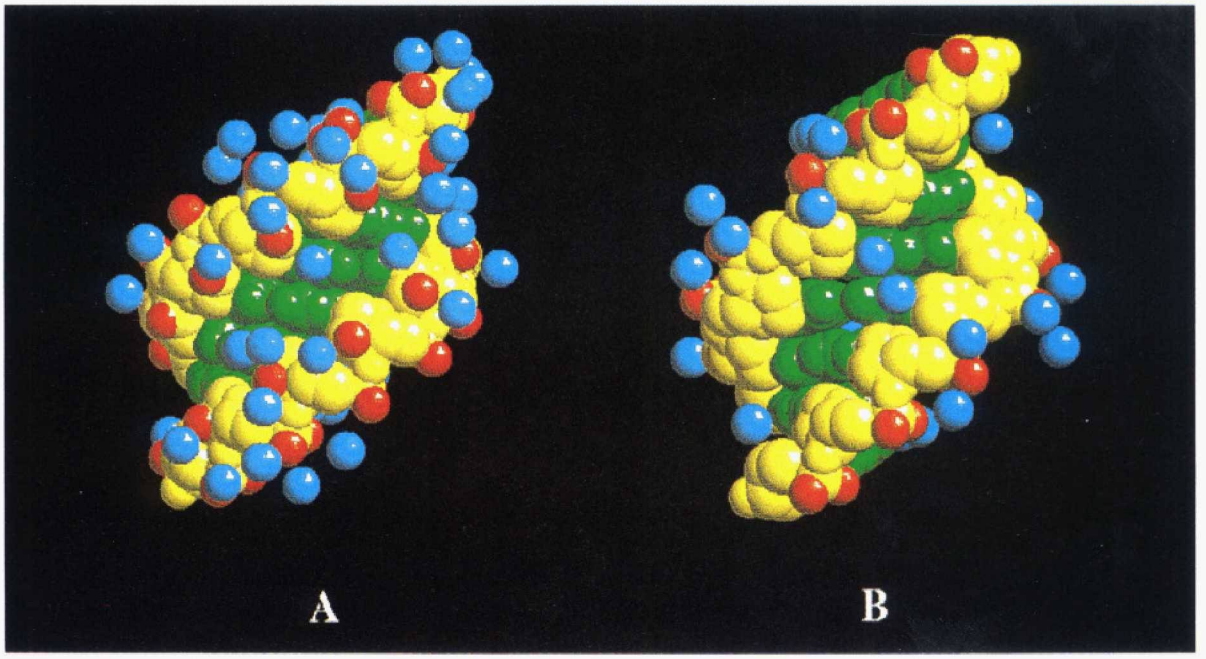

FIGURE 3: Minor groove hydrations in the rhombohedral $[r(C_4G_4)]_2$ duplex (A) and the A-DNA duplex $[d(C_4G_4)]_2$ (B) (Eisenstein & Shakked, 1995). Phosphate and 2′-oxygen atoms are in red, the remaining sugar−phosphate backbone atoms are in yellow, base atoms are in green, and water molecules are in cyan. Only first-shell water molecules with distances to RNA or DNA atoms of less than 3.4 Å are shown.

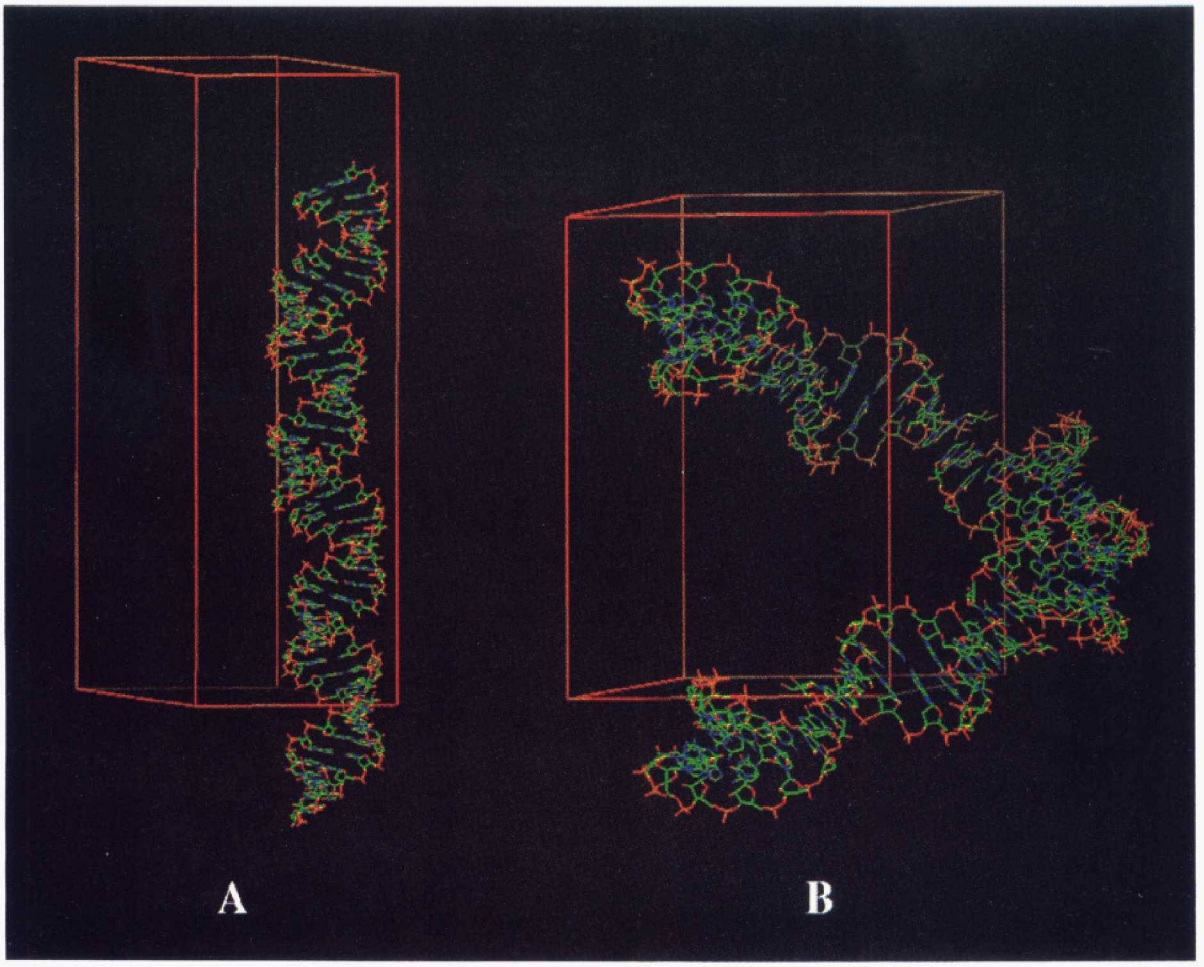

FIGURE 4: Generation of a continuous double helix by adjacent octamers in the rhombohedral crystal (A). The origin of the unit cell is at the front bottom left, and the *z*-axis is vertical. Generation of a right-handed superhelix by adjacent octamers in the hexagonal crystal (B). The origin of the unit cell is at the front bottom right, and the *z*-axis is vertical.

DNA double helix with sequence d(GGGCGCCC) was demonstrated to undergo drastic conformational changes in different lattices and upon cooling (Shakked *et al.*, 1989), a hexagonal modification at low temperature displaying a

conformation not unlike the one found in the case of our two RNA octamers.

Hydration. An important contribution to the higher thermodynamic stability of the RNA duplex relative to the DNA duplex is based on the steric and stereoelectronic consequences of the 2′-hydroxyl group in RNA. Possibly more important in terms of stability than these factors is the improved sugar−phosphate backbone and base hydration in the minor groove brought about by the ribose 2′-hydroxyl group. Now, for the first time, with the crystal structures of both, an RNA and a DNA A-type double helix with identical sequence at hand, we can compare their minor groove hydration patterns and obtain an estimate for the stability gains resulting from the additional hydrogen bond accepting and donating function in the ribose moiety. Figure 3 depicts views into the minor grooves of the rhombohedral RNA duplex and the A-DNA duplex, both with sequence C_4G_4. Apart from a few water molecules coordinated to phosphate groups and bases, the DNA minor groove is essentially dry. To a certain extent this lack of hydration can be attributed to the stacking of terminal base pairs from two neighboring molecules into the minor groove. The extensive hydration of this groove in the RNA is directly related to the presence of the ribose 2′-hydroxyl groups; these are engaged in a total of 25 hydrogen-bonding interactions. All 2′-oxygens are coordinated to two water molecules on average except for the two terminal cytidines from one strand. This region displays relatively high thermal mobility in the crystal, and it was therefore decided to exclude water molecules from crystallographic refinement which were tentatively assigned to it. Importantly, in the majority of base pairs water molecules link the 2′-hydroxyl groups with the O2 oxygen of cytidines and the N3 nitrogen of guanidines. The more hydrophobic nature of the DNA minor groove may explain the interaction modes between duplexes observed in the crystal lattices of A-DNA octamers. It appears that RNA duplexes generally prefer an end-to-end stacking arrangement over base pair−minor groove interactions, possibly due to the altered polarity of the groove as a consequence of the 2′-hydroxyl groups and the water molecules bound to them. Undoubtedly, their systematic hydration provides an important contribution to the overall stability of the RNA duplex and, in addition, is likely to be of importance for the stability and the selectivity of RNA−protein interactions.

Crystal Packing. Rhombohedral and hexagonal crystals of the RNA octamer C_4G_4 grow under distinct conditions which differ in buffer type and pH as well as in the precipitation agent. Adjacent double helices in the rhombohedral crystal generate infinite columns (Figure 4A), and in the hexagonal crystal they define a right-handed superhelix (Figure 4B). Therefore, contacts between helices in both forms occur primarily between their terminal base pairs. However, the stacking modes in the two crystals deviate; in the rhombohedral lattice duplexes are stacked head to tail (Figure 5A), creating a more or less continuous double helix, interrupted only by the missing phosphate groups between octameric segments (Figure 4A). In the hexagonal form, helices are stacked head to head (Figure 5B) with consequently discontinuous major and minor grooves (Figure 4B).

There is a fundamental difference between the interaction modes in the crystal lattice for octameric A-type DNA duplexes and the ones for the RNA duplexes in the present study. Without exception, DNA interactions involve van der Waals contacts of terminal base pairs with the shallow minor grooves of neighboring duplexes, rather than the stacking interactions seen with the RNAs. The minor groove of the $d(C_4G_4)$ duplex is somewhat narrower than the minor grooves of the RNA duplexes, and it is possible that this a consequence of the differing interduplex contacts in the two cases. In the rhombohedral lattice RNA duplexes are more tightly packed side by side than in the hexagonal lattice (Figures 6 and 7). The tighter packing in the case of the rhombohedral crystal is also evident from the comparisonof the volumes per base pair for the two forms (Table 1). As a consequence of the short distance between stacks in the rhombohedral crystals, individual duplexes are tightly interlocked, inserting their backbones into the minor grooves of neighbors (Figure 6). Thus, hydrogen bonds are formed between phosphate groups and 2′-hydroxyl groups rimming the minor grooves of neighboring helices at close contact sites, and in addition, several water molecules mediate contacts between atoms of two adjacent duplexes both within and between stacks. In the hexagonal lattice tubes of RNA duplexes are separated by a larger distance, and no backbone−minor groove contacts between neighboring duplexes are consequently found (Figure 7).

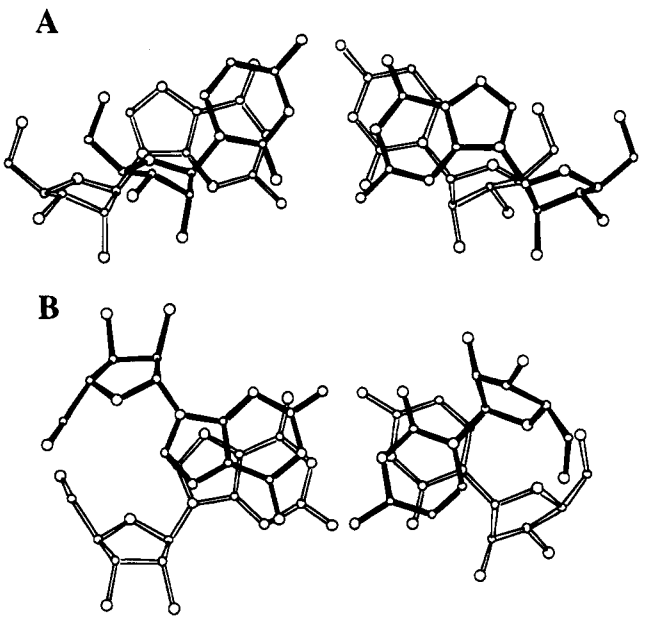

FIGURE 5: Stacking between terminal base pairs of adjacent duplexes in the rhombohedral (A) and hexagonal (B) crystal forms of $r(C_4G_4)$. The projections are along the normal to the best plane through the top base pair (filled bonds). In the rhombohedral crystal stacking is of the 5′,3′/5′,3′ type, and the local twist angle is 4° (based on a helix axis defined by two stacked octamer duplexes). In the hexagonal crystal stacking is of the 5′,5′/3′,3′ type with the stacked base pairs related via a crystallographic 2-fold rotation axis (horizontal in the paper plane).

Biological Implications. Our finding that the conformations of an RNA duplex in two distinct crystallographic environments are nearly identical is consistent with the similarities between the corresponding stem regions of transfer RNA^{Phe} molecules in the monoclinic (Westhof & Sundaralingam, 1986) and the orthorhombic crystal form (Westhof *et al.*, 1988). This lends support to the view that regular stem regions in large RNA molecules serve mainly as rigid structure-stabilizing units. The RMS deviations

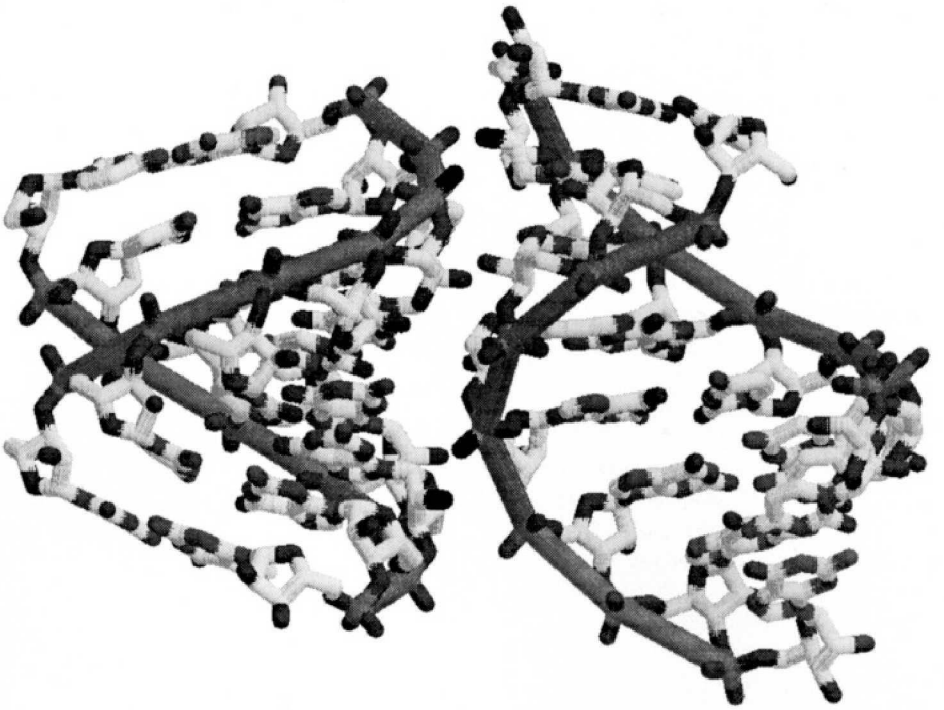

FIGURE 6: Backbone−minor groove interactions between adjacent duplexes in the rhombohedral crystal lattice. Each double helix inserts one of its backbones into the minor groove of an adjacent helix and vice versa. Phosphate and 2′-oxygen atoms involved in direct interduplex hydrogen-bonding contacts are highlighted in black.

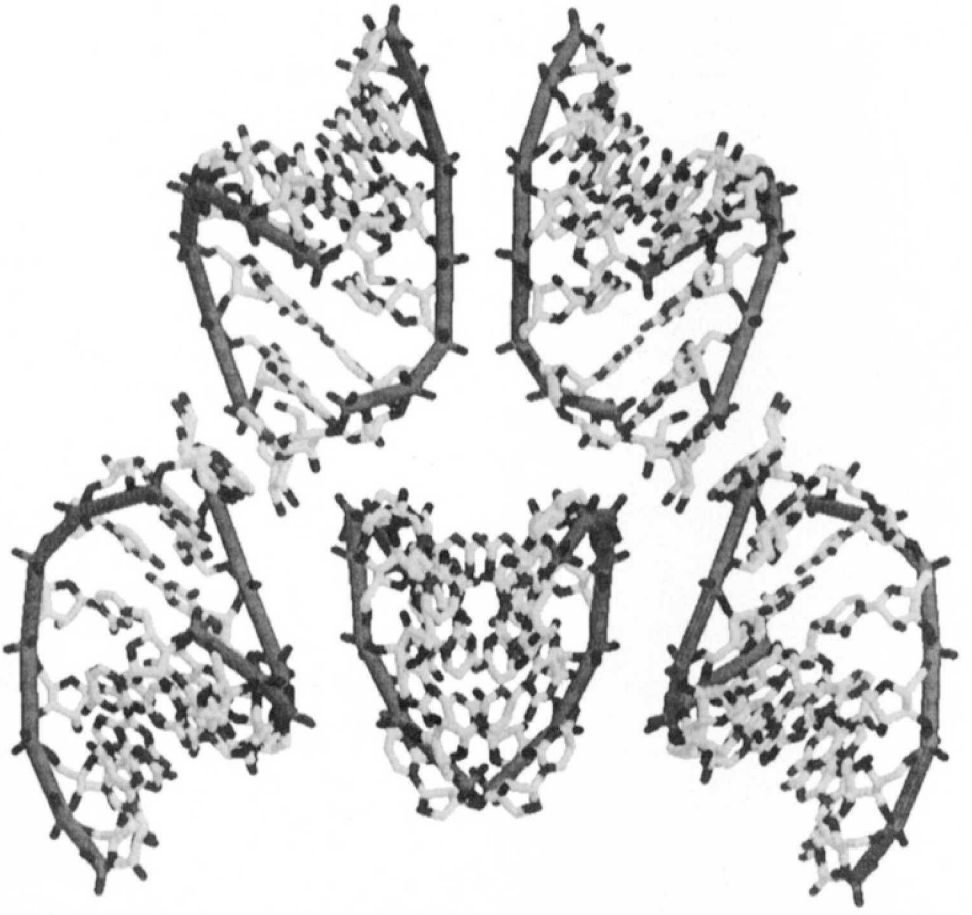

FIGURE 7: Packing arrangement in the hexagonal crystal lattice. Stacking interactions between terminal base pairs constitute the closest lattice contacts; there are no backbone−minor groove interactions as in the rhombohedral crystal.

between individual such stems (acceptor, D, anticodon, T) in the two tRNA crystal forms are all below 0.70 Å. The comparison between the conformations of $tRNA^{Asp}$ in its free state and complexed with its cognate synthetase revealed drastic conformational changes of a stem region only for the anticodon duplex section adjacent to the loop (Cavarelli *et*

al., 1993). There are currently only very few detailed three-dimensional structures of RNA oligonucleotides (Dock-Bregeon *et al.*, 1988; Holbrook *et al.*, 1991; Cruse *et al.*, 1994; Leonard *et al.*, 1994; Baeyens *et al.*, 1995) and protein−RNA complexes (Rould *et al.*, 1989; Ruff *et al.*, 1991; Biou *et al.*, 1994; Oubridge *et al.*, 1994, Valegård *et al.*, 1994). Nevertheless, the close correspondence of RNA stem conformations in different crystallographic environments and the results of the present work may indicate that such regions will not be altered drastically by RNA-binding proteins. By comparison, proteins have been observed to induce massive conformational changes in their double-stranded DNA targets in order to form a sequence-specific protein−DNA interface [e.g., Schultz *et al.* (1991), Kim, J. L., *et al.* (1993), Kim, Y., *et al.* (1993), and Klimasauskas *et al.* (1994)]. Evidently, the RNA itself takes on a much more active role in the protein−nucleic acid recognition process compared with DNA. Thus, base mismatches, single- or multiple-base bulges, loops, and a flurry of other secondary structure elements (Wyatt & Tinoco, 1993) can serve the specific interaction of proteins with RNA (Frankel *et al.*, 1991; Weeks & Crothers, 1991; Musier-Forsyth *et al.*, 1991; Oubridge *et al.*, 1994, Valegård *et al.*, 1994). As more three-dimensional structures of RNA fragments are being determined, the roles of base sequence, hydration, ion binding, and other factors constituting the fundaments of the catalytic properties of RNA will become better understood.

ACKNOWLEDGMENT

We thank Dr. Fritz K. Winkler (Hoffmann LaRoche Ltd., Basel) for help with data collection and processing.

REFERENCES

Baeyens, K. J., De Bondt, H. L., & Holbrook, S. R. (1995) *Nature Struct. Biol. 2*, 56.

Biou, V., Yaremchuk, A., Tukalo, M., & Cusack, S. (1994) *Science 263*, 1404.

Brünger, A. T., Kuriyan, J., & Karplus, M. (1987) *Science 235*, 458.

Cavarelli, J., Rees, B., Ruff, M., Thierry, J.-C., & Moras, D. (1993) *Nature 362*, 181.

Collaborative Computational Project, Number 4 (1994) *Acta Crystallogr., Sect. D 50*, 760.

Cruse, W. B. T., Saludjian, P., Biala, E., Strazewski, P., Prangé, T., & Kennard, O. (1994) *Proc. Natl. Acad. Sci. U.S.A. 91*, 4160.

Dickerson, R. E. (1992) in *Methods in Enzymology* (Lilley, D. M. J., & Dahlberg, J. E., Eds.) Vol. 211, pp 67−111, Academic Press, San Diego.

Dock-Bregeon, A. C., Chevrier, B., Podjarny, D., Moras, D., deBear, J. S., Gough, G. R., Gilham, P. T., & Johnson, J. E. (1988) *Nature 335*, 375.

Egli, M. (1994) in *Structure Correlation* (Bürgi, H.-B., & Dunitz, J. D., Eds.) pp 705−749, VCH Publishers, New York.

Egli, M., Portmann, S, Tracz, D., Workman, C., & Usman, N. (1995) *Acta Crystallogr., Sect. D* (in press).

Eisenstein, M., & Shakked, Z. (1995) *J. Mol. Biol. 248*, 662.

Frankel, A. D., Mattaj, I. W., & Rio, D. C. (1991) *Cell 67*, 1041.

Haran, T. E., Shakked, Z., Wang, A. H.-J., & Rich, A. (1987) *J. Biomol. Struct. Dyn. 5*, 199.

Holbrook, S. R., Cheong, C., Tinoco, I., Jr., & Kim, S.-H. (1991) *Nature 353*, 579.

Jain, S., & Sundaralingam, M. J. (1989) *J. Biol. Chem. 264*, 12780.

Kennard, O., & Hunter, W. N. (1991) *Angew. Chem., Int. Ed. Engl. 30*, 1254.

Kim, J. L., Nikolov, D. B., & Burley, S. K. (1993) *Nature 365*, 520.

Kim, Y., Geiger, J. H., Hahn, S., & Sigler, P. B. (1993) *Nature 365*, 512.

Klimasauskas, S., Kumar, S., Roberts, R. J., & Cheng, X. (1994) *Cell 76*, 357.

Leonard, G. A., McAuley-Hecht, K. E., Ebel, S., Lough, D. M., Brown, T., & Hunter, W. N. (1994) *Structure 2*, 483.

Lipanov, A., Kopka, M. L., Kaczor-Grzeskowiak, M., Quintana, J., & Dickerson, R. E. (1993) *Biochemistry 32*, 1373.

Musier-Forsyth, K., Usman, N., Scaringe, S., Doudna, J., Green, R., & Schimmel, P. (1991) *Science 253*, 784.

Navaza, J. (1994) *Acta Crystallogr., Sect. A 50*, 157.

Oubridge, C., Ito, N., Evans, P. R., Teo, C.-H., & Nagai, K. (1994) *Nature 372*, 432.

Quigley, G. J., Teeter, M. M., & Rich, A. (1978) *Proc. Natl. Acad. Sci. U.S.A. 75*, 64.

Ramakrishnan, B., & Sundaralingam, M. (1993) *J. Biomol. Struct. Dyn. 11*, 11.

Rould, M. A., Perona, J. J., Söll, D., & Steitz, T. A. (1989) *Science 246*, 1135.

Ruff, M., Krishnaswamy, S., Boeglin, M., Poterszman, A., Mitschler, A., Podjarny, A., Rees, B., Thierry, J. C., & Moras, D. (1991) *Science 252*, 1682.

Saenger, W. (1984) *Principles of Nucleic Acid Structure*, pp 242−252, Springer, New York.

Scaringe, S. A., Francklyn, C., & Usman, N. (1990) *Nucleic Acids Res. 18*, 5433.

Schultz, S. C., Shields, G. C., & Steitz, T. A. (1991) *Science 253*, 1001.

Shakked, Z., Guerstein-Guzikevich, G., Eisenstein, M., Frolow, F., & Rabinovich, D. (1989) *Nature 342*, 456.

Usman, N., Egli, M., & Rich, A. (1992) *Nucleic Acids Res. 20*, 6695.

Valegård, K., Murray, J. B., Stockley, P. G., Stonehouse, N. J., & Liljas, L. (1994) *Nature 371*, 623.

Wang, A. H.-J., Fujii, S., van Boom, J. H., & Rich, A. (1982) *Proc. Natl. Acad. Sci. U.S.A. 79*, 3968.

Weeks, K. M., & Crothers, D. M. (1991) *Cell 66*, 577.

Westhof, E., & Sundaralingam, M. (1986) *Biochemistry 25*, 4868.

Westhof, E., Dumas, P., & Moras, D. (1988) *Acta Crystallogr., Sect. A 44*, 112.

Wyatt, J. R., & Tinoco, Jr., I. (1993) in *The RNA World* (Gesteland, R. F., & Atkins, J. F., Eds.) pp 465−496, Cold Spring Harbor Laboratory Press, Cold Spring Harbor, NY.

BI950565L